SLAC-PUB-3089
UR846/C00-3065-353
March 1983
(T/E)

A Comparison of the Deep Inelastic Structure Functions of Deuterium and Aluminum Nuclei*

A. Bodek, N. Giokaris

Department of Physics and Astronomy
University of Rochester, Rochester, NY 14627 USA

W. B. Atwood, D. H. Coward

Stanford Linear Accelerator Center
Stanford University, Stanford, CA 94305 USA

D. L. Dubin, M. Breidenbach,[1] J. E. Elias,[2] J. I. Friedman,
H. W. Kendall, J. S. Poucher,[3] and E. M. Riordan[4]

Physics Department and Laboratory for Nuclear Science
Massachusetts Institute of Technology, Cambridge, MA 02139 USA

Abstract

We have measured the deep inelastic electromagnetic structure functions of deuterium and aluminum nuclei. The kinematic dependence of the ratio of aluminum and deuterium structure functions is similar to the dependence of the ratio of steel and deuterium structure functions, and provides further evidence for the distortion of the quark momentum distributions of nucleons bound in a nucleus.

(Submitted to Physical Review Letters)

---

* Work supported by the Department of Energy, contracts DE-AC03-76SF00515 (SLAC), DE-AC02-76ER13065 (Rochester) and DE-AC02-03069 (MIT).

[1] Present address: Stanford Linear Accelerator Center, Stanford, CA 94305

[2] Present address: Fermilab, Batavia, IL 60510

[3] Present address: Bell Labs, Holmdel, NJ 07733

[4] Present address: Cheshire Books, 514 Bryant St., Palo Alto, CA 94301

In a recent communication[1] we reported the observation of a significant difference between the inelastic structure functions of steel and deuterium nuclei extracted from deep inelastic electron scattering data. The electron data confirmed the effect observed at higher momentum transfers by the European Muon Collaboration[2] (EMC). Within the quark parton model, the deviation of the ratio F_2^{Fe}/F_2^D from unity suggests a distortion of the quark distributions for nucleons bound in a nucleus. A study of the quark distributions in nuclei for various nuclei over a wide range of x and Q^2 could be highly useful in establishing the origin of this nuclear effect. We report here on $\sigma_{A\ell}/\sigma_D$, the ratio of differential cross sections <u>per nucleon</u> for nucleons bound in aluminum and for nucleons bound in the deuteron, measured over a large range of x. This ratio can be interpreted (under certain assumptions[1]) as the structure function ratio $F_2^{A\ell}/F_2^D$ where F_2 is the structure function that exhibits approximate scaling in x.

The experiment[3,4] was designed to measure deep inelastic electron scattering from hydrogen and deuterium over a large range of x in order to extract the proton and neutron structure functions. Differential cross sections from the scattering of electrons from hydrogen, deuterium and an aluminum empty target replica were measured at the Stanford Linear Accelerator Center (SLAC) using the SLAC 8-GeV spectrometer. We have recently analysed the empty target data in order to compare aluminum and deuterium cross sections. We comment briefly on those points related to this comparison.

Differential cross sections were measured at laboratory scattering angles (θ) of 18°, 26° and 34°, for several values of incident energies E ranging from 4.5 to 20 GeV and a range of scattered electron energies E'. The liquid H_2 and D_2 target cells were cylinders 7 cm in diameter with 0.003" thick aluminum walls. The empty-target contributions were measured using an aluminum empty-target replica with 0.018" thick wall,[5] chosen so that the amount of radiator in the aluminum target replica was nearly the same as that for the full targets. Thus the radiative corrections for the full and empty targets were essentially identical[6,7]. The rates measured with the empty-target replica were divided by the ratio of the wall thicknesses (6.0) before subtraction from the full-target rates. The electron contribution from background processes such as π° decay and electron pair production was determined by reversing the spectrometer polarity and measuring the charge symmetric positron cross sections. This background, which was subtracted from the electron cross section, was significant (<30%) only at the lowest values of E'/E. The measurements with hydrogen, deuterium and aluminum targets were interspersed to minimize systematic errors.

The measured raw cross sections were corrected for the minute acceptance differences between aluminum and deuterium targets[8]. A small correction (0.3% to 1.7%) was applied for the neutron excess in aluminum (using fits to neutron and proton data[4]) so that $\sigma_{A\ell}$ as reported here is the cross section <u>per nucleon</u> for a hypothetical aluminum nucleus with <u>equal</u> number of neutrons and protons. The radiative corrections[1,9] changed the $\sigma_{A\ell}/\sigma_D$ ratio by less than 1%. Values of $\sigma_{A\ell}/\sigma_D$ as a function of the variable $x=Q^2/2M\nu$ and the variable[10] $\xi=2x/(1+\sqrt{1+4M^2x^2/Q^2})$ are given in Table 1 and shown in Figure 1a. The values were obtained by calculating the ratios at all kinematic points with $W\gtrsim1.8$ GeV/c^2 and forming weighted averages[11] over small intervals in x or ξ. Here $W=(M^2+2M\nu-Q^2)^{\frac{1}{2}}$ is the final state invariant mass, M is the mass of the proton, $\nu=E-E'$ is the energy transfer, and $Q^2=4EE'\sin^2\theta/2$ is the invariant square of the four momentum transfer[12].

The random errors arising from counting statistics dominate the typically 1% error in the cross sections obtained by adding in quadrature the errors from random fluctuation (e.g. flux monitors, liquid target densities and rate dependent effects). Only random errors are shown in Figures 1a and 1b. Most systematic errors in the cross sections (solid angle, incident and scattered electron energy calibration, monitor calibration) and most uncertainties in the radiative corrections cancel in the ratio $\sigma_{A\ell}/\sigma_D$. The number of nucleons/cm^2 in the liquid deuterium target was determined[4] to an accuracy of ±1.1%. The number of nucleons/cm^2 in the aluminum empty target replica was measured to an accuracy of ±2% by weighing sections cut out of the target, measuring the areas with a planimeter, measuring the thickness with a micrometer, and measuring the density with a pycnometer. We estimate an overall systematic error of ±2.3% in the $\sigma_{A\ell}/\sigma_D$ ratio. The systematic error in the ratio from radiative corrections is estimated to be less than 1%. The low x points ($x<0.2$) have additional systematic uncertainties due to backgrounds from lower energy electrons in the beam halo. These backgrounds were estimated from "hole runs" taken with a target that consisted of a 2" hole in a thick aluminum frame. Systematic errors of 100% were assigned to the magnitude of the halo background subtractions. These errors (given in the caption of table 1) are added linearly to the errors of the low x data points.

The data show a significant x dependent difference between aluminum and deuterium cross sections in a manner opposite to that expected from Fermi motion effects. The Fermi motion corrections have been calculated by Bodek and Ritchie[13] by extending the Atwood and West technique for the deuteron[14]. The calculations employ non-relativistic wave functions, and use off-mass-shell relativistic kinematics for energy-momentum conservation. These calculations agree with the results of Frankfurt and Strickman[15] who have calculated the corrections using a parton model approach which satisfies parton model sum rules. Within the quark parton model the x distributions, at sufficiently large momentum transfers, determine the momentum distribution of the quarks in the nucleon. Thus the data suggest that the quark momentum distributions in a nucleon bound in aluminum become distorted. Figure 1a also shows $\sigma_{A\ell}/\sigma_D$ for $\langle Q^2\rangle \approx 1.2 (\mathrm{GeV/c})^2$ as measured by Stein et al.,[9] and the $\sigma_{A\ell}/\sigma_D$ ratio as measured in photoproduction[16] ($Q^2=0$). The three experiments taken together indicate that at small x and small Q^2 the ratio is significantly reduced suggesting that nuclear shadowing[17] effects, which are presumably higher twist effects in the language of QCD, may be important.

Figure 1b shows our recent measurements[1] of σ_{Fe}/σ_D in a similar Q^2 range, and the EMC data[2] at much higher Q^2. Also shown are values[9] for σ_{Cu}/σ_D for $\langle Q^2\rangle \approx 1.2 (\mathrm{GeV/c})^2$ as well as σ_{Fe}/σ_D from photoproduction data[16]. These data from heavier targets taken together also indicate that at low Q^2 shadowing effects may cancel some of the nuclear enhancement at low x. These additional Q^2 dependent nuclear higher twist effects, like higher twist effects in the nucleon, are expected to be small at large values of Q^2. Therefore, the extraction of Λ_{QCD} from structure function data taken with nuclear targets at high values of Q^2 may not be affected by these terms.

We have performed a linear fit the $\sigma_{A\ell}/\sigma_D$ ratios for our data in the range $0.2 \le x \le 0.6$ ($\langle Q^2\rangle = 5.35 (\mathrm{GeV/c})^2$) and obtain an intercept at x=0 of 1.11±0.02±0.023 (where the second error is systematic) and a slope of -0.30±0.06. A similar fit to our σ_{Fe}/σ_D results[1] (see figure 1b) over the range $0.2 \le x \le 0.6$ ($\langle Q^2\rangle = 6.55 (\mathrm{GeV/c})^2$) yields an intercept at x=0 of 1.15±0.04±0.011 and a slope of -0.45±0.08. Our slope for steel is consistent with the slope of -0.52±0.04±0.21 reported by the EMC collaboration.[2] The fitted slopes, which are not affected by overall normalization uncertainties, indicate that the nuclear distortion in aluminum and steel exhibit a similar trend.

The understanding of the mechanisms responsible for the distortion of the structure functions of nucleons bound in a large nucleus has been the subject of several recent theoretical papers. These include ideas such as six quark bags[18], pions and quasipions in nuclei[19], delta resonances in nuclei[20], diquark states[21] and percolation of quarks fron nucleon to nucleon in a large nucleus[22]. The data indicate that there are three interesting regions (a) the low x region where shadowing may be important at low Q^2 (b) the intermediate x region where quark distributions in nuclei become distorted and (c) the high x region where Fermi motion is important. The theoretical understanding of these effects is still in a very qualitative state and new experiments designed to investigate further the structure functions of various nuclei are needed.

We wish to express our gratitude and appreciation to all members of the Stanford Linear Accelerator Center. We thank Dieter Walz and Jack Nicol (from SLAC) for help with the target measurements and Nick Ray (from Rochester) for programming support. This work was supported in part by Department of Energy Contracts DE-AC02-76ER13065 (Rochester), DE-AC02-03069 (MIT) and DE-AC02-76F00515 (SLAC).

References

1. A. Bodek et al., Phys. Rev. Lett. 50, 1431 (1983).
2. J. J. Aubert et al., Phys. Lett. 123B, 275 (1983).
3. A. Bodek et al., Phys. Rev. Lett. 30, 1087 (1973); SLAC experiment E49B referred to as experiment A in Ref. 4.
4. A. Bodek et al., Phys. Rev. D20, 1971 (1979).
5. Type 5052-0 aluminum, measured density 2.65 g/cm^3 (±2%), radiation length = 9.0 cm, mean A = 27.02, mean Z = 13.02. Average composition 2.5% Mg (A=24.32), 0.25% Cr(A=52), 0.75% Max(Si, Fe, Cu, Mn, Zn), remainder Al(A=26.98). Note that the number of nucleons/cm^2 was directly measured (see text).
6. In units of 10^{-2} radiation lengths, the value used for the average amount of radiator before scattering was 0.588 and 0.518 for deuterium and aluminum respectively. The average amounts after the scattering at angles of 18°, 26° and 34° were 1.117, 1.114, and 1.109 for deuterium and 1.035, 1.065, and 1.111 for aluminum, respectively.
7. A. Bodek, Nucl. Inst. and Meth. 109, 603 (1973).
8. The 7 cm target is almost a point source for the 8 GeV spectrometer. The acceptance for the empty target was smaller than the acceptance for the full target by 0.07%, 0.13% and 0.15% for data taken at 18°, 26° and 34° respectively. Note that a 14 cm target and a larger spectrometer aperture were used in Ref. 1.
9. S. Stein et al., Phys. Rev. D12, 1884 (1975).
10. O. Nachtmann, Nucl. Phys. B63, 237 (1973); H. Georgi and H. D. Politzer, Phys. Rev. D14, 1829 (1976).

11. A. Bodek, Nucl. Inst. and Meth. 117, 613 (1974); errata 150, 367 (1978); A. Bodek SLAC-TN-74-2, 1974 (unpublished).

12. The mean Q^2 of the data shown in Table 1 is 1.9, 2.2, 2.4, 2.7, 2.4, 3.1, 3.8, 4.2, 5.2, 5.2, 7.0, 6.8, 7.5, 8.7, 8.3, 11.8, 11.4, 13.8 and 20.1 $(GeV/c)^2$ for x bins starting at 0.075 and ending at 0.863 respectively.

13. A. Bodek and J. L. Ritchie, Phys. Rev. D23, 1070 (1981); D24; 1400 (1981).

14. W. B. Atwood and G. B. West, Phys. Rev. D7, 773 (1973).

15. L. I. Frankfurt and M. I. Strickman, Nucl. Phys. B148, 107 (1979).

16. D. O. Caldwell et al., Phys. Rev. Lett. 42, 553 (1979); Phys. Rev. D7, 1362 (1973); A. M. Eisner, "Proceedings of the 1979 International Symposium on Lepton and Photon Interactions, Fermilab, Aug. 1979, p.448, ed. T. B. W. Kirk and H. D. I. Abarbanel.

17. G. Grammer and J. D. Sullivan, "Nuclear Shadowing of Electromagnetic Processes", in Electromagnetic Interactions of Hadrons, Vol. 2, p.195, ed. A. Donnachie and G. Shaw, Plenum Press, 1978.

18. R. L. Jaffe, Phys. Rev. Lett. 50, 228 (1983); H. J. Pirner and J. P. Vary, UNI-HD-83-02; C. E. Carlson and T. J. Havens, Stony Brook preprint (1983).

19. C. H. Llewellyn Smith, Oxford Preprint 18/83; M. Ericson and A. W. Thomas, CERN TH-3553 (1983).

20. J. Szwed, Cracow preprint TPJU-1/83 (Jagellonian University).

21. J. D. Bjorken, private communication.

22. G. Baym, Physica 96A, 131 (1979).

Table Caption

Table 1: $\sigma_{A\ell}/\sigma_D$ as a function of x and ξ. The ratio expected from Fermi motion is from Ref. 13. The data have been corrected for the small neutron excess in aluminum, and have not been corrected for Fermi motion effects. In order to correct for Fermi motion, the $\sigma_{A\ell}/\sigma_D$ ratios should be divided by the numbers in column 3. The mean Q^2 is given in footnote 12. Only random errors are shown. The normalization error is estimated to be ± 2.3%. There are additional point to point systematic errors of 6%, 4%, 3%, 2% and 1% that apply to the first five data points respectively.

Table 1

x or ξ	$\sigma_{A\ell}/\sigma_D$ x bins	Fermi Motion	$\sigma_{A\ell}/\sigma_D$ ξ bins
0.075	0.863±0.132	1.030	0.863±0.132
0.10	1.018±0.040	1.031	1.018±0.040
0.125	1.060±0.032	1.032	1.060±0.032
0.15	1.061±0.030	1.033	1.061±0.030
0.175	1.062±0.026	1.034	1.064±0.022
0.213	1.040±0.013	1.035	1.038±0.013
0.263	1.047±0.015	1.038	1.052±0.014
0.313	1.019±0.013	1.040	1.006±0.014
0.363	0.992±0.018	1.041	1.006±0.016
0.413	0.984±0.019	1.042	0.950±0.021
0.463	0.971±0.025	1.035	0.979±0.023
0.513	0.928±0.031	1.027	0.917±0.031
0.563	0.967±0.030	1.010	0.987±0.035
0.613	0.992±0.034	0.982	0.956±0.032
0.663	0.934±0.045	0.941	0.958±0.040
0.713	0.954±0.040	0.862	0.890±0.098
0.763	0.919±0.089	0.775	1.141±0.098
0.813	1.167±0.113	0.632	1.010±0.505
0.863	1.010±0.505	0.448	-----------

Figure Caption

Figure 1: $\sigma_{A\ell}/\sigma_D$ (a) and σ_{Fe}/σ_D (b) versus x. Only random errors are shown. Point to point systematic errors have been added linearly (outer bars) where applicable. The normalization errors of ±2.3% and ±1.1% for $\sigma_{A\ell}/\sigma_D$ (E49B) and σ_{Fe}/σ_D (E87) respectively are not included. All data for $W \gtrsim 1.8$ GeV are included. The data have been corrected for the small neutron excess and have <u>not</u> been corrected for Fermi motion effects. The curve indicates the expected ratio if Fermi motion effects were the only effects present (Ref. 13). High Q^2 σ_{Fe}/σ_D data from EMC (Ref. 2), low Q^2 σ_{AL}/σ_D and σ_{Cu}/σ_D data from Ref. 9, and photoproduction σ_{AL}/σ_D and σ_{Fe}/σ_D data from Ref. 16 are shown for comparison. The systematic error in the EMC data is ±1.5% at x=0.35 and increases to ±6% for the points at x=0.05 and x=0.65.

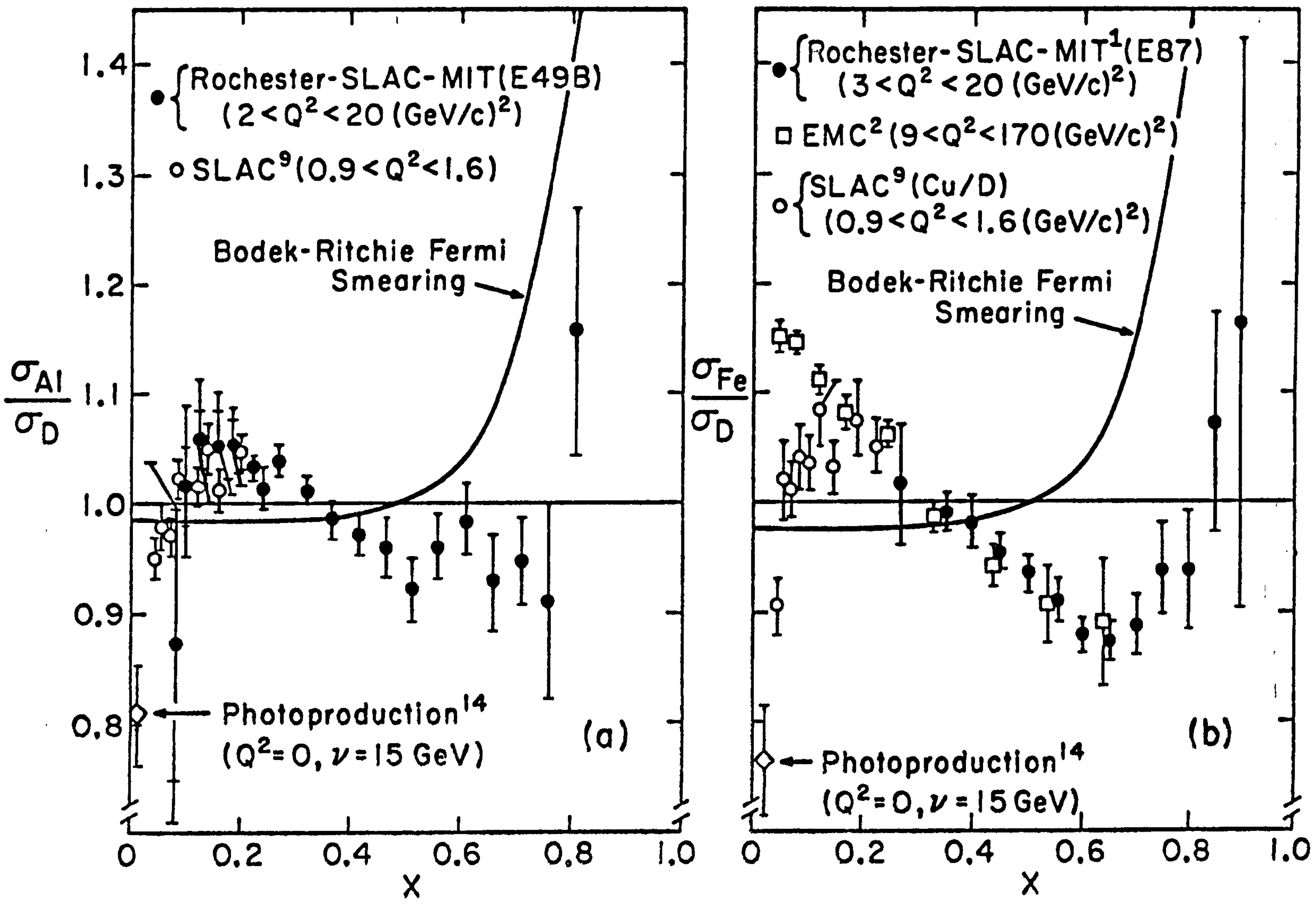

(a)
σ_{Al}/σ_D
1.4
1.3
1.2
1.1
1.0
0.9
0.8
● Rochester-SLAC-MIT(E49B) ($2<Q^2<20$ (GeV/c)^2)
○ SLAC^9 ($0.9<Q^2<1.6$)
Bodek-Ritchie Fermi Smearing
Photoproduction^{14} ($Q^2=0$, $\nu=15$ GeV)
0
0.2
0.4
0.6
0.8
1.0
X
(b)
σ_{Fe}/σ_D
● Rochester-SLAC-MIT^1(E87) ($3<Q^2<20$ (GeV/c)^2)
□ EMC^2 ($9<Q^2<170$(GeV/c)^2)
○ SLAC^9 (Cu/D) ($0.9<Q^2<1.6$ (GeV/c)^2)
Bodek-Ritchie Fermi Smearing
Photoproduction^{14} ($Q^2=0$, $\nu=15$ GeV)
0
0.2
0.4
0.6
0.8
1.0
X